New Journal of Physics
The open-access journal for physics

Charge transfer from core-excited argon adsorbed on clean and hydrogenated Si(100): ultrashort timescales and energetic structure

S Lizzit[1], G Zampieri[2,9], K L Kostov[3], G Tyuliev[4], R Larciprete[5], L Petaccia[1], B Naydenov[6] and D Menzel[7,8,10]

[1] Sincrotrone Trieste S.C.p.A. S.S.14 Km. 163.5, 34012 Trieste, Italy
[2] Centro Atomico Bariloche and Instituto Balseiro, Comision Nacional de Energia Atomica, 8400-Bariloche, Argentina
[3] Institute of General and Inorganic Chemistry, Bulgarian Academy of Science, 1113 Sofia, Bulgaria
[4] Institute of Catalysis, Bulgarian Academy of Science, 1113 Sofia, Bulgaria
[5] CNR Institute of Complex Systems, via Salaria Km 29.3, 00016 Monterotondo Scalo Rome, Italy
[6] Trinity College Dublin, Dublin 2, Ireland
[7] Physik-Dept. E20, Techn. Univ. München, 85748 Garching, Germany
[8] Fritz-Haber-Institut der MPG, Dept. CP, D-14195 Berlin, Germany
E-mail: dietrich.menzel@ph.tum.de

New Journal of Physics **11** (2009) 053005 (17pp)
Received 18 February 2009
Published 19 May 2009
Online at http://www.njp.org/
doi:10.1088/1367-2630/11/5/053005

Abstract. Using the well-established core hole-clock method under resonant Auger Raman conditions we have measured the charge transfer (CT) times for the 4s electron on $2p_{3/2}$ core excited Ar atoms adsorbed on Si(100). The influences of the doping (p- or n-type), surface condition (clean or covered with monohydride) and varied excitation energy have been examined. The data for the Si–H surfaces are most extensive and distinct and undisturbed by background or losses. The CT times, which are identical for n- and p-type materials, are found to be about 2 fs at resonance. They show a distinct energy dependence when broadly tuning the excitation energy through the Ar core resonance. The CT times on clean Si(100), for which the data are not as extensive, are shorter

[9] Member of CONICET of Argentina.
[10] Author to whom any correspondence should be addressed.

 © IOP Publishing Ltd and Deutsche Physikalische Gesellschaft

by a factor of ∼2 compared to the Si–H surfaces and again about the same for n- and p-type Si(100). The unexpectedly short CT times found, as well as the energetic structure seen, are discussed in terms of possible influences of the projected surface electronic structure of Si(100) in the energy range of the Ar 4s electron, and of other explanations. Theoretical modeling would be highly desirable.

Contents

1. Introduction and method	**2**
2. Experimental	**4**
3. Results and analysis	**5**
4. Discussion	**13**
5. Summary and conclusions	**15**
Acknowledgments	**16**
References	**16**

1. Introduction and method

The many important changes induced in the structure, state, dynamics and reactivity of molecules by binding them to surfaces are due to the coupling of their discrete states to the structured continuum represented by the solid surface, for the electronic as well as the vibrational structures. As to electronic coupling, charge exchange and charge transfer (CT) are already very important aspects in the ground state of adsorbate systems. Even more obvious is the role that the rates of CT—connected with energy transfer and delocalization of excitation—play in the *electronically excited* states of adsorbed molecules. Surface photochemistry, or more generally electronically induced surface processes, can be distinctly different from those of similar gas phase species due to this possibility of charge and energy transfer between adsorbate and substrate (see e.g. [1, 2]). From indirect arguments and from calculations it has long been derived that the rates of such processes must be of the order of a few fs or even faster [1, 2]. Many surface processes, including charge and energy transfer, have been investigated in the past decade by laser pump–probe measurements (LPP) on very short timescales (see e.g. [3]–[5] and references therein). However, the range around or below 1 fs has started to become accessible by such methods only recently [3]–[6]. So the possibility to access such short timescales by using the lifetime of localized core excitations as a clock (core-hole-clock, CHC, method) ([7]–[9] and work cited therein) is very welcome. We note that LPP and CHC experiments appear to look at somewhat different processes, even if taking into account that an atom of nuclear charge Z with a core hole closely corresponds to a ground state atom of nuclear charge $Z + 1$ (‘equivalent core approximation’). These differences are not a subject of the present paper.

In the CHC approach, absorption of a soft x-ray photon from synchrotron radiation (SR) produces a well-defined adsorbate core excitation localized on a specific atom; and the decay spectra of the core hole are measured. In the energy range below 1–2 keV the main core hole decay (CD) channel is Auger decay, so that the measurement of the decay electrons provides information on the decay processes; the surface sensitivity of slow electrons is an added asset. The presence or absence of the excited electron on the adatom at the instant of its

CD induces a shift between the decay spectra in the two situations, so that the former can be distinguished by these spectra. The relative strengths of the two channels—CD *before* or *after* CT to the substrate—can then be derived from the ratio of the integrals over the two types of spectra [7]–[9]. In early measurements [10], the existence or absence of a difference between the decay spectra after resonant and nonresonant (continuum) core excitation of an adsorbate was used as indication of the CT rate relative to the CD rate. When narrow bandwidth SR with sufficient intensity became available at SR sources, an improved version of this 'core hole clock' method became possible [7]–[9], [11, 12]. In this a resonant core excitation is induced under so-called Auger resonant Raman (ARR) conditions (i.e. the exciting bandwidth is below the lifetime width of the core excitation), and the decay spectra are measured while the narrow excitation band width is tuned through the resonance. The mentioned two contributions in the spectra which are shifted against each other, due to CD *before* or *after* delocalization—mainly into the substrate; see discussion below—of the locally excited electron can then be separated by their different responses to the changing photon energy. With sufficient signal quality the usually overlapping multi-peaked spectra can be disentangled: for the 'true Auger' contribution (CT before CD) the electron kinetic energies stay constant as the photon energy is varied; for the 'Raman' contribution (CD before CT) the difference between photon energy and electron kinetic energy (KE) (i.e. the binding energy) stays constant. As can be shown by a rate approach, the ratio of their integrated intensities gives directly the ratio of the two characteristic rates or decay times [7]–[9], [11, 12], so that the CT time can be derived for a known core hole lifetime. This principle has become especially fruitful by the ready availability of third generation SR sources with their small photon bandwidths at good intensity. This not only allows more reliable procedures to separate the two sets of spectra, but also makes the (albeit narrow) variation of the primary excitation possible. The derived information on the change of the CT time with the exact energetic position of the excited electron that can be transferred contains important information about the basic mechanism of the transfer and the controlling factors [7]–[9], [13].

With this method a number of investigations have been conducted on Ar adsorbed on various metal surfaces (Pt(111) [11], Ru(0001) [12], Cu(111), Ag(111), Ni(111) [13], Cu(100) and Cu(111) [14]). On Ru(0001) Ar has also been studied on well-defined adsorbates as spacer layers, leading to a wide variation of CT times [7]. Ar is a useful test atom because of its easily accessible $2p_{3/2} \rightarrow 4s$ core level excitation and its weak adsorption bond which leads to CT times on metals of the order of 1–5 fs. Since the $2p_{3/2}$ core hole lives about 6 fs, it is very well suited as a clock in this time range [13]. It should be noted that the core-excited Ar atom (in the following Ar c^* or $c^{-1}4s$) is equivalent to a K atom to good approximation, and the 4s electron is initially localized on it. In many of the cited systems the dependence on the exact excitation energy clearly showed that the mechanism is neither simple tunneling through a barrier into a receiving structureless reservoir, nor is it influenced by an Auger Raman-type effect [7, 9, 13]. Rather, the type and density of the surface projected substrate states accessible for the transferred electron appear to be decisive to interpret the found CT times, and there may even be no real barrier at the relevant energy; the latter conclusion has been corroborated theoretically [15]. For clean Ru(0001) [16] as well as for Cu(111) and Cu(100) [14] calculations on this basis have recently been presented which bear out these statements. Also, very fast CT processes (down to a few 100 as) have been demonstrated for strongly coupled adsorbates, for chemisorbed CO [17], and recently for chemisorbed S on Ru(0001) [18]. In the latter case,

a theoretical treatment also arrived at good agreement and a conclusive picture connecting to the substrate band structure [18].

So far, only metal surfaces have been investigated in this detail. The picture described above is that CT is governed by the overlap of the orbital of the excited electron on the c* adsorbate with the available empty surface-projected substrate states of suitable symmetry, so that for the same adatom (here Ar) the surface band structure is expected to be decisive. It is then likely that large bandgap materials will indeed exhibit a barrier and show very slow CT, as already seen for Ar on top of one monolayer of Xe and one monolayer of Ar [7] on a metal. It appeared interesting, then, to look at a substrate with in-between properties and check the timescale as well as whether the predominance of band structure features is visible there as well. We have therefore selected Si(100) surfaces. To check a possible influence of the overall charge distribution, we have looked at both n-type and p-type Si(100). To provide information on the influence of saturating the surface states and of a kind of spacer layer, we have not only looked at the clean surface, but also at that with a monohydride layer. Preliminary versions of some of the results have been used as examples in a recent tutorial review [9].

This paper is structured as follows. First we give a short description of the techniques used for sample preparation, data collection, and data analysis. This is followed by a description of the results which are discussed in the final chapter.

2. Experimental

The measurements have been done at the SuperESCA beamline of the SR source ELETTRA in Trieste/Italy. The ultrahigh-vacuum chamber, with a base pressure of 5×10^{-11} mbar, is equipped with an argon-ion sputter gun, a quadrupole mass spectrometer, a rear-view low-energy electron diffraction (LEED) system, and a double pass electron energy analyzer with 150 mm mean radius for each hemisphere and a 96-channel detection system. The Si samples were mounted on a low-temperature manipulator with four degrees of freedom, which allows fast cooldown to 80 K using liquid nitrogen, or to 15 K using liquid helium as the coolant. Two types of silicon samples, n-Si(100) (phosphorus doped, 1–4 Ohm cm) and p-Si (100) (boron doped, 4.5–6 Ohm cm) were used to test a possible influence of doping. They were mounted on a tantalum plate by a multilayer bonding technique via thin tungsten and silver interlayers [19]. The samples were heated by electron bombardment, and their temperature was measured with a chromel–alumel thermocouple spotwelded to the back of the tantalum plate. The surfaces were cleaned by repeated cycles of Ar^+(1 keV) sputtering with both grazing and 45° incidence, both at low temperatures and at 800 K, with subsequent annealing to 1150 K and slow cooling ($\sim$20 K s^{-1}) to 400 K. XPS showed no contamination (C 1s, O 1s) after several cleaning cycles and the high resolution Si 2p spectrum was representative of a clean surface; the LEED pattern revealed sharp spots indicative of a well-ordered 2×1 surface. The monohydride surfaces were produced by exposing the clean surfaces to hydrogen from a hot tungsten tube atomizer at 650 K followed by cool-down to 460 K and anneal at 650 K, resulting again in a good (2×1) LEED pattern and Si 2p XPS with well-distinguished core level-shifted components.

After pretreatment the crystals were cooled to about 15 K by liquid He. In some measurements the sample temperature was higher due to a deterioration of the crystal bonding to the holder which in the extreme led to charge-up of the samples in some experiments. These cases that concern some results for clean Si will be pointed out below; results with noticeable charge-up were eliminated. Argon was adsorbed by exposing the crystal to 3 L

(1 Langmuir = 10^{-6} Torr s) argon gas at base temperature from the background or with an equivalent amount through a dosing micro-channelplate. Then the crystals were warmed to 35 K to desorb multilayers and leave a full monolayer of Ar behind (which would desorb around 40 K). These conditions had been established by fast XPS of Ar 2p. XPS of Si 2p and of C 1s and O 1s were taken to check the cleanliness and freedom from impurities. For the Ar-covered surfaces, Ar 2p XPS was used to check that no depletion of the Ar layer by the irradiation during measurement had taken place (in the cases of deteriorated bonding of the crystal to the holder, the Ar coverage was found to be somewhat reduced). The photon beam impinged in the surface normal so that the E-vector was in the surface plane; the emitted electrons were measured at 70° from the surface normal, optimizing the surface contribution. During measurements the sample was scanned in order to avoid beam damage or desorption of the adsorbed Ar.

3. Results and analysis

Figure 1 (insert) shows the x-ray absorption spectrum (XAS) monitored by partial electron yield (PEY) spectroscopy (cutoff energy 120 eV to eliminate Si 2p contributions) in the range of the Ar $2p_{3/2} \rightarrow 4s$ resonance which lies at 244.4 eV and has a halfwidth of ~0.6 eV, for a monolayer of Ar on a n-Si(100)–H sample (Si–H in the following). The gas phase absorption peak, obtained under identical conditions and with the same apparatus, is also shown. It is seen that the two resonance energies agree within resolution, so that there is no uncertainty in photon energy calibration. The photon bandwidth was about 40 meV, so that ARR conditions were clearly fulfilled. The XA spectra from Ar-covered n-type and p-type Si(100)–H were identical within the error limits. Decay spectra for Si–H were taken through the entire region of the resonance (from 243.2 to 245.1 eV) at 100 meV intervals, as well as below and above the resonance at some selected photon energies for background determination and calibration purposes. In addition to the Ar gas phase resonance shown, the photon energies were calibrated by gas phase measurements on N_2 and Ne.

The main body of figure 1 shows a set of decay spectra across the resonance (for better clarity, only a part of the measured spectra are shown; the corresponding photon energies are marked in the absorption spectrum of the insert), for a monolayer of Ar on n-Si–H. The individual spectra were normalized to the background ~1 eV above the Ar 3s peak to eliminate small changes of the photon intensity. Then the (low) background due to unspecific secondary electrons, Auger peaks excited by second-order light, and some substrate-related structure was determined as explained below and subtracted. The decay spectra in figure 1 are shown on a KE scale, so that Auger peaks stay constant while Raman and photoelectron peaks shift to higher energies with increasing photon energy. The reference level is the Fermi level of the mounting. At the right the Ar 3s photoelectron peak is visible whose KE shifts with exciting photon energy as expected (the binding energy, BE, is constant). In principle, it could contain a resonant part from participant decay of the Ar $2p_{3/2} \rightarrow 4s$ resonance, in addition to direct photoemission. However, already the raw data (not shown here; see [9]) suggest that this contribution is negligibly small. After normalizing the spectra to the background above the Ar 3s line to remove intensity changes of the source, the intensity of the 3s peak becomes constant within the accuracy of the measurements. So indeed the participant contribution is negligible. This is to be expected since the participant contribution in the gas phase is only about 8%. As the Raman contribution is between 10 and 30% of the total signal (see below), the participants are indeed expected to be between 1 and 2% of the total decay signal. In fact, this is an independent

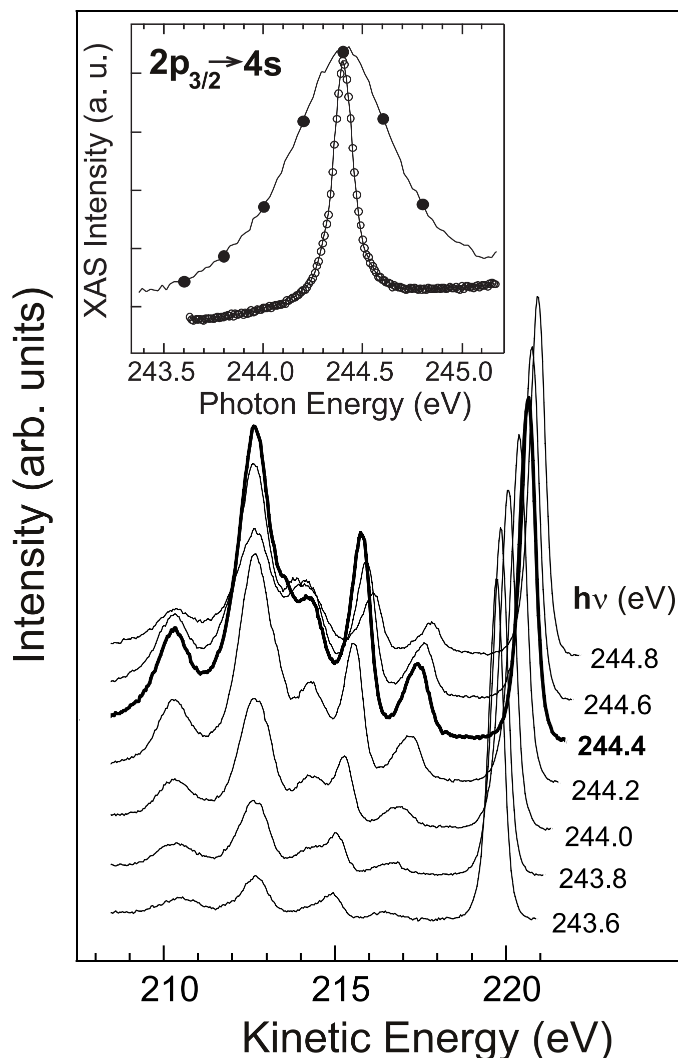

Figure 1. Inset: resonant absorption peak for the $2p_{3/2} \rightarrow 4s$ excitation of an Ar monolayer on a n-Si(100)–H surface, measured by partial electron yield at a photon resolution of 40 meV (continuous line). The narrower gas phase absorption peak measured in the same machine and under the same conditions of undulator and spectrometer is also shown (empty circles). Main figure: decay spectra for these excitations at the photon energies shown (highlighted with full circles in the inset), plotted as a function of the KE of the decay electrons, so that Auger peaks do not shift with changed photon energy. The high peak on the right is the Ar 3s photoelectron peak. For clarity, only part of the measured spectra is shown.

semiquantitative corroboration of the small Raman contributions and consequently of the very fast timescales involved (see below).

Without any analysis it is obvious that the peaks at KE of ∼210.8 and ∼213 eV are Auger peaks and that the shifting peaks at KE of ∼216.5 and ∼218 eV at resonance are Raman peaks; between these two sets contributions from shifting and nonshifting components can be

discerned. Compared to Ar decay spectra on several metals published earlier (Ru [7, 12], Pt [11], Ni, Cu, Ag [13, 14]) these decay spectra are clearer, sit on a much lower background, and are essentially free of 'satellite' (better 'loss') contributions at low KE. We believe the higher background and the loss regions seen on metals to be due to coupled low-energy electron–hole excitations, which are missing here on the semiconductor surface with saturated surface states. The spectra for n-Si(100) and p-Si(100) were virtually identical, except for a shift of about 1 eV of the kinetic energies of the decay peaks which was also observed for the Si levels. This is compatible with flatband conditions due to the presence of a saturation surface photovoltage that arises at our rather high photon intensity. However, we note that this was only seen at 15 K, our measurement temperature; at room temperature the Si core levels moved to low/high BE for n/p doping by about 0.5 eV—a clear indication of band bending.

Figure 2 shows decay spectra for clean n-Si(100) (Si–cl in the following), and, as an inset, the absorption resonance. The latter is slightly shifted (by ∼90 meV) against Ar on Si–H and the Ar atom (figure 1, inset), and somewhat broader than on Si–H (∼0.7 versus 0.6 eV). Absorption and decay spectra were again the same on p- and n-type samples. Here a more limited energy range was investigated because of the sample bonding difficulties mentioned. The definition of the decay peaks is not as clear, and the background is somewhat higher. The poorer signal/noise ratio is mainly due to the somewhat lower Ar coverage because of the mentioned cooling problems. The higher background and larger peak width is likely due to coupled excitations between surface states, and possibly to a larger defect concentration on clean Si(100); the particularly high homogeneity attainable for hydrogenated Si surfaces known from vibrational spectroscopy (albeit using special etching techniques for best results) [20], might also contribute to the better peak definition on Si–H.

Nevertheless, considerably different partitioning between the two channels can be seen in the decay spectra of figure 2, compared to figure 1. This is even more obvious in the comparison of decay spectra at resonance (figure 3). Obviously on Si–cl the Raman range is weaker, so that the CT times must be shorter. Furthermore, the peaks are less distinct and have a somewhat larger background, as already mentioned and discussed. A clear observation is the shift of the Ar 3s photoemission peak by ∼0.2 eV to lower BE for Si–cl. The distances from this peak to the Raman peaks are identical in the two cases. The Auger peaks are even shifted by 0.6 eV to lower BE (higher KE) for the Si–cl. This correlation of shifts of 1-hole (or 2-hole 1-electron; photoemission and Raman) and of 2-hole (Auger) peaks which are related by a factor of 3 shows that both these shifts are due to somewhat different hole screening on the two surfaces [21]. As expected, the holes in Ar on Si–cl are better screened than on Si–H. It appears (and is borne out by the fitting analysis, see below) that the Auger peaks for Si–cl are broadened compared to Si–H (in fact the Raman and photoemission peaks on Si–cl are also slightly broadened compared to those on Si–H). Together with the screening differences just pointed out this makes it likely that inhomogeneities of the Ar/Si–cl layers act mainly to lead to inhomogeneities of screening. However, some of that may also be due to the less well-defined Ar coverage and to coupled small losses (see above). Because of these effects the range of photon energies with acceptable signal strengths and without charging influences (see above) was smaller for clean Si, so that the analysis is somewhat less certain. Again there was no significant difference between n- and p-type silicon, apart from the shift of the KE scale seen if there clearly was no charging. We want to emphasize that this conclusion about negligible influence of doping is independent of any possible uncertainties of the reference level, since the decay spectra can be directly compared.

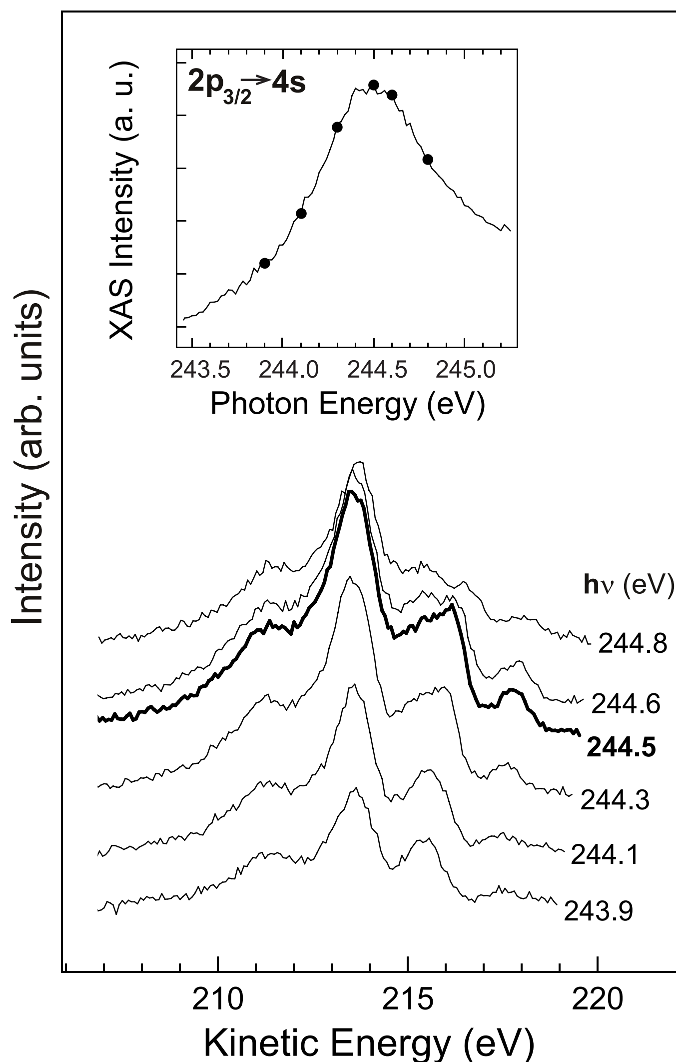

Figure 2. Inset: resonant absorption peak for the $2p_{3/2} \rightarrow 4s$ excitation of an Ar monolayer on a clean n-Si(100) surface, measured by partial electron yield at a photon resolution of 40 meV (continuous line). The resonance maximum is shifted by 90 meV to higher energy compared to gas phase and Ar/Si–H (figure 1). Main figure: decay spectra for these excitations at the photon energies shown (highlighted with full circles in the inset), plotted as a function of the KE of the decay electrons, so that Auger peaks do not shift with changed photon energy.

In order to extract the CT times, the spectra have to be decomposed into Raman and Auger contributions after subtraction of the small background. The two lower Auger and the two higher Raman peaks are well separated, so that their energies can be easily determined; only in the overlap region is the decomposition critical. In order to accomplish this with high accuracy, the background unrelated to the decay spectra has to be determined and subtracted. Figure 3 shows the procedure used, for the spectra at resonance for both Si–H and Si–cl. The largest part of this type of background is due to unspecific secondaries at constant BE coming from the Si substrate

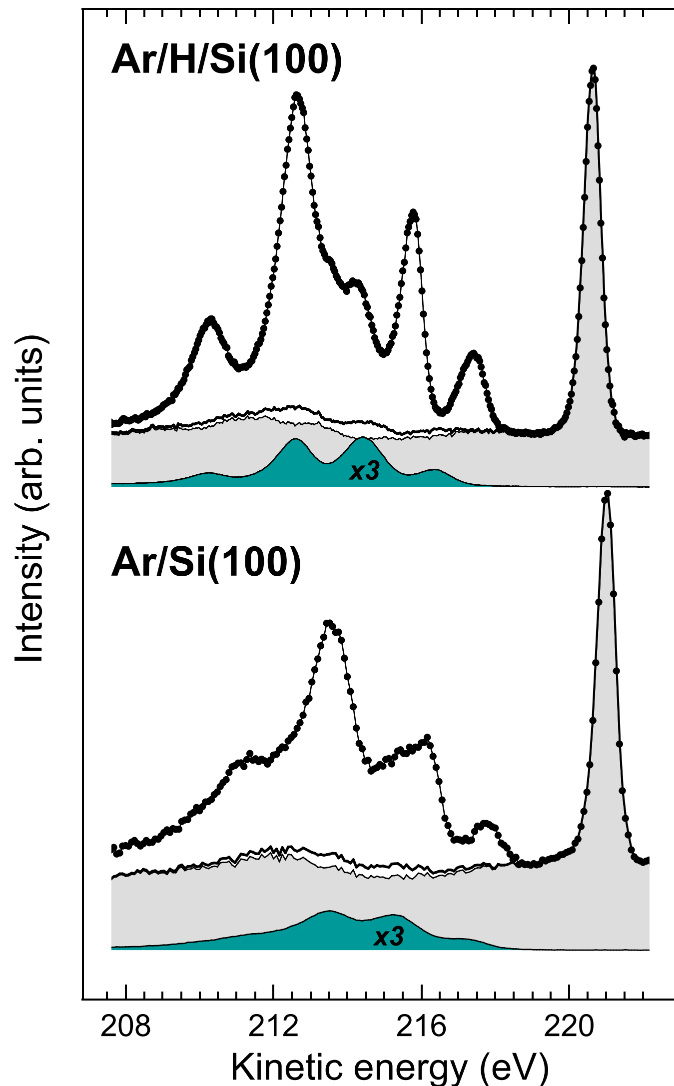

Figure 3. Demonstration of the background determination for both types of surfaces and differentiation into unspecific background (with constant BE) and contributions of continuum excitation of Ar Auger electrons caused by second-order light of the monochromator (with constant KE). Fat points and curves: measured decay spectra at resonance. Thin line with light gray shaded area: background measured at 232 eV. Peaked structure at bottom with dark shaded area: Auger spectrum by second-order light of the monochromator (3×), determined as described in the text. Fat line: total background, determined for the photon energy at resonance, i.e. sum of the spectra highlighted in light and dark gray.

as well as from the Ar 3s photoemission peak; the Auger contributions due to second-order light of the monochromator (at constant KE) are smaller but potentially more disturbing as they are peaked. It should be noted that these Auger contributions are quite different from those from 4s CT, since they also contain the decay of $2p_{1/2}$ excitations. They were determined from Auger

spectra measured at 272 eV (i.e. essentially in the continuum region), scaled by measurements below the 2p thresholds in first order. These contributions are displayed in figure 3.

All spectra were treated first with this background subtraction and then subjected to a strongly constrained fitting procedure with two functions for the Auger and Raman parts, respectively, plus a linear (i.e. unspecific) inelastic background of the decay spectra (as shown in figure 3, the latter contributions were very small). Very good fits to all spectra on H-terminated Si(100) (n- and p-type) were possible while keeping *all* lineshape parameters (peak locations, widths and relative heights; Gaussian and Lorentzian contributions) *constant* for *all* photon energies and *all* conditions. The two fitting functions are shown in figure 4 (top); they consist of a sum of 5 Voigt functions, nonshifting for the Auger, and 5 equally shifting for the Raman peaks [22] on top of a linear background (only three each are apparent here because some multiplets are not resolved due to the broadening seen). The constant spacings between the peaks agree well with the spacings obtained for gas phase atoms ([22] and work cited therein). The Raman peaks are narrower by about a factor 1.8 than the Auger peaks, again suggesting that a large part of the final state widths is due to inhomogeneous screening. The quality of the fits down to low kinetic energies demonstrates clearly that distinct losses (‘satellites’) have no noticeable influence for Ar on Si–H.

For fitting the data of the clean Si spectra (figure 4, bottom), the *same* set of energy spacings and relative intensities were used. The only change necessary was to use larger width parameters (about factors 1.6 and 1.2 larger for the Auger and Raman peaks, respectively compared to Si–H). While the fits were not as perfect due to the broader peaks, higher noise and additional background, they were still good. In particular, the increase of width parameters was sufficient to account for the spectral features down to low kinetic energies, as clear from figure 4 (bottom). No assumption of broader loss features was necessary to get the demonstrated fits.

We then integrate over the individual spectra and obtain the ratio of the integrated Raman/Auger intensities which according to a simple rate approach [7]–[9], [11, 13] is proportional to the ratio of the corresponding lifetime widths, or to the inverse of the ratio of the lifetimes:

$$N_{1(2)} = \int I_{1(2)}(E)\mathrm{d}E,$$
$$N_1/N_2 = k_1/k_2 = \tau_2/\tau_1,$$
$$\tau_{\mathrm{CT}} = (N_{\mathrm{Raman}}/N_{\mathrm{Auger}})\tau_{\mathrm{ch}},$$

where $N_{1(2)}$ are the integrated intensities of the competing paths 1 or 2 (CT and CD, respectively, corresponding to Auger and Raman parts of the spectra), $k_{1(2)}$ are the corresponding rate constants and $\tau_{1(2)}$ are the time constants. This is fully equivalent and simpler than the often used treatment with Raman fractions [7]–[9].

Figure 5 shows all the results. As to the accuracy in the CT times, there is no rational way to derive error bars for the entire procedure used, in particular since statistical errors are expected to be only a small part of the errors, and systematic errors (from background subtraction, losses, etc) are likely to be more important. These problems have not been big here due to the high quality of the data; they were further minimized by our careful and strongly constrained data treatment described above. In order to check the reliability of the fit procedures to get an estimate for the errors involved, the fits have been repeated independently by different investigators for the range of acceptable parameters, under the stringent conditions summarized above, taking into consideration the range given by the signal/noise ratio (high around resonance but

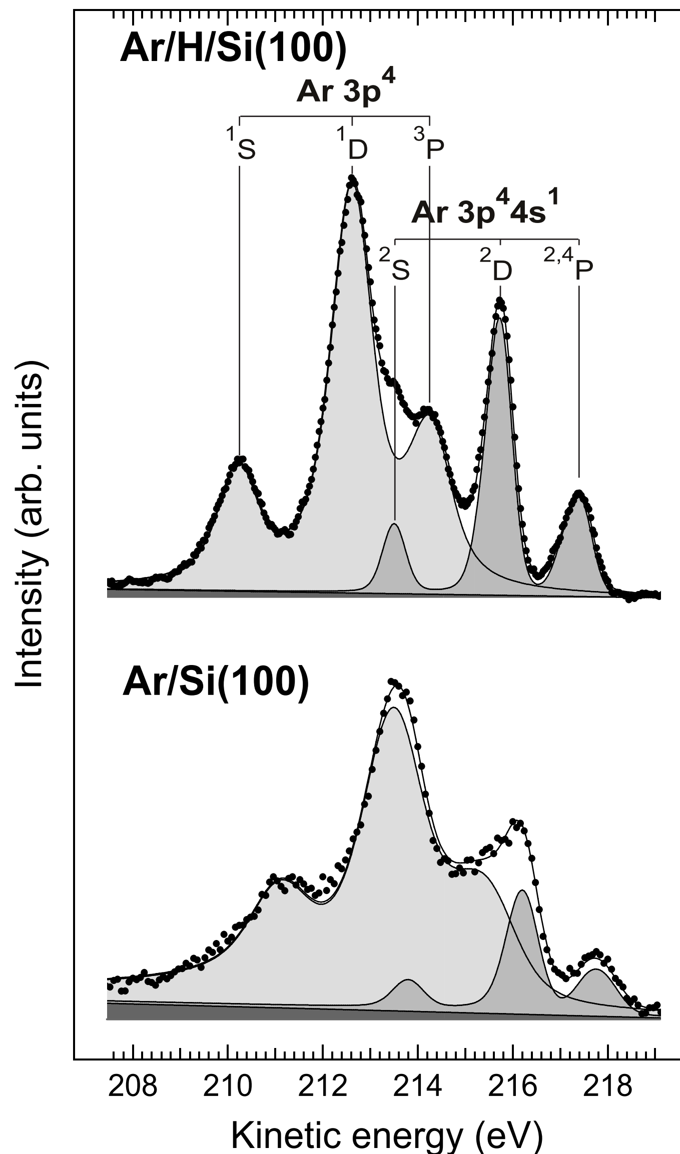

Figure 4. Demonstration of fits for the two types of surfaces, Si–H and Si–cl, to differentiate Raman and Auger parts of the spectra after the background subtraction shown in figure 3 and further subtraction of the low linear background coming from the fit (black wedges on bottom). The line between the dots is the result of the fit with the fit functions shown. The assignment to decay peaks known from the gas phase is indicated. For details see text.

decreasing away from it). We find that for the Si–H data, the error stemming from the fit is smaller than ±0.06 fs around the resonance maximum (±0.4 eV); farther from the resonance the errors are somewhat larger, and in particular at energies more than 0.6 eV above the resonance contributions from decay of the Ar $2p_{1/2}{}^{-1}$ 4s excitation begin to influence the fit quality. For Si–cl the errors are larger even around the resonance, as expected. Figure 5 gives error bars estimated on these grounds.

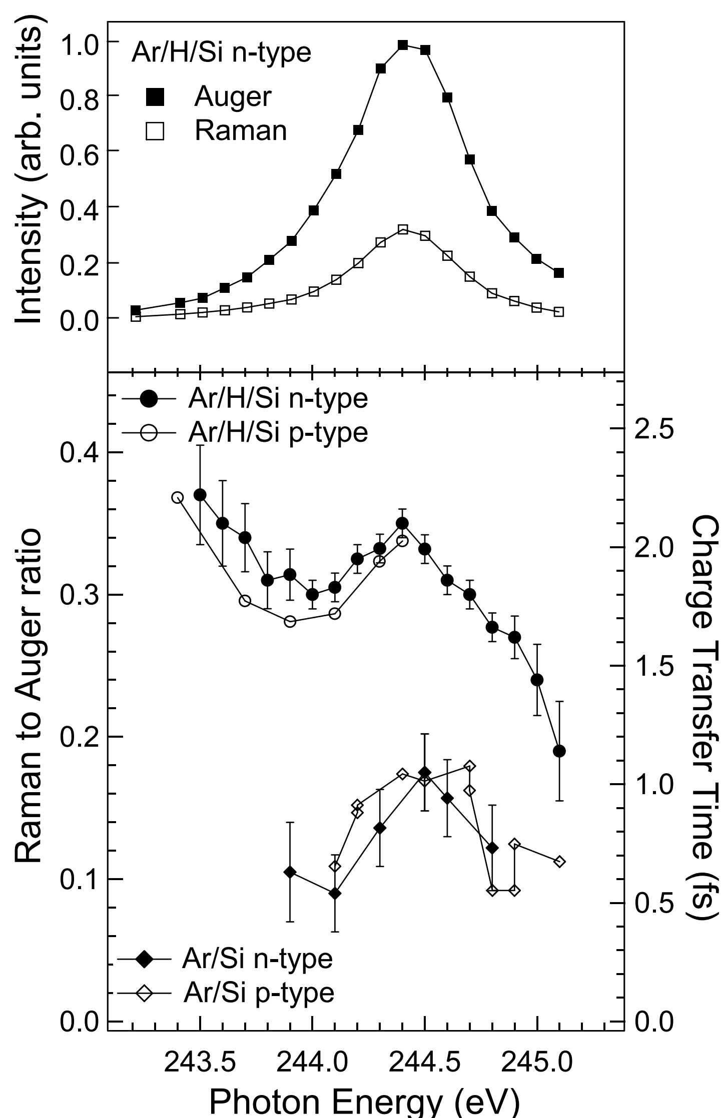

Figure 5. Top: integrals of Raman and Auger parts of the decay spectra as function of photon energy, for the case n-Si–H. Bottom: compilation of all results for the ratios of integrated Raman/Auger contributions (left ordinate) and the corresponding CT times (right ordinate), for the systems as indicated in the figure. Procedures and considerations leading to the error bars shown (n-type each only for clarity) are given in the text.

The first feature of the results is the unexpectedly short range of CT times, even taking the largest error bars. Also, distinct structure as a function of excitation energy is observed for Si–H. Furthermore, unquestionably the general range of the time ratios on the clean surfaces is shifted to shorter times compared to that of the Si–H surfaces. This means that on Si–cl the delocalization of the Ar 4s electron is faster (roughly by a factor of 2) than on Si–H. Because of the mentioned larger errors for Si–cl, we would not claim that in this case the energetic structure seen is trustworthy if only these results existed. However, since the structure agrees well with

that clearly obtained for the Si–H surfaces, it is possible that the same excited state structure is observed here as well around the resonance.

The comparison of n- and p-Si shows that the Ar c^{-1}4s level is tied to the vacuum level; this agrees with expectation and with the results on the other Ar systems. Comparison of the resonance energy (244.4 eV) to the binding energy of the Ar $2p_{3/2}$ level relative to the vacuum level (determined to ∼247.0 eV) shows that the center of the Ar 4s electron level is at ∼2.6 eV below the vacuum level. This is an approximate determination because of the difficulties in reliably localizing the Fermi level of Si samples relative to the valence band top and the vacuum level [23], and as it assumes that the screening of the $2p_{3/2}$ hole by the 4s electron on the same atom is identical to the polarization screening for its continuum excitation. This latter assumption has been made in all previous analyses. Because of these uncertainties this determination may contain a (pessimistically estimated) error up to about ±0.3 eV. It should be noted that energy shifts between different spectra in our data are accurate to better than 0.05 eV. The rather large possible error in the absolute calibration does not influence this relative accuracy. Also our finding that doping is unimportant is not influenced by these calibration uncertainties.

4. Discussion

The most interesting aspects of our data are the short CT times seen, and their quite distinct structure with excitation energy at least for Si–H. The found CT times are in the range seen on metal surfaces [7]–[14], which is surprising—intuitively one might expect longer CT times on a semiconductor.

Before discussing these points we have to ascertain that the delocalization times found are indeed due to coupling to the substrate, as has been implicitly assumed. It should be noted that, while for large molecules with high polarizability it is possible that the excited electron in the lowest unoccupied molecular orbital (LUMO) is delocalized within the layer—the condition for this is that the excitonic energy of the localized c^* state can be cancelled by the polarization screening of the ‘bare’ core hole by the surrounding medium—this is not possible for core-excited Ar. This is a consequence of the negative electron affinity of Ar: the 4s energy on a ground state atom is at least 4 eV above that of the core-excited Ar, while the polarization screening can bring back only about 1.5 eV. So it is expected that the process determining the localized lifetime of the 4s electron is the transfer to the substrate. Indeed, the cited earlier theoretical analyses for Ar and S on metals [14, 16, 18] have clearly shown that for a constant source orbital the surface-projected band structure of the substrate into which delocalization occurs has a strong influence on the CT times. The short CT times for core-excited Ar on clean Si(100), which are similar to the fastest times seen on transition metals, would then suggest that there must be a high surface projected empty density of states in the range of the Ar c^*4s resonance; or in molecular terms, a well-fitting surface orbital of suitable symmetry overlapping strongly with the Ar^* 4s orbital.

The lack of influence of the doping type shows that the CT is not influenced by the electronic properties and carrier densities between valence band maximum and conduction band minimum. This is not surprising in view of the higher energy of the investigated excited electron. The general similarity of the shapes for clean and H-covered Si suggests that in the energy range about 2.5 eV below the vacuum level and up, H-adsorption does not change the density of states much. Then the factor of 2 between the two types of surfaces must be mainly due to a decoupling

effect and consequently decreased overlap. The weaker coupling is also seen in the decreased screening of 1 and 2 h states on Si–H evident from the energy shifts (see above). Whether this decoupling is mainly due to an increased distance of the adsorbed Ar on Si–H, as in the case of rare gas spacer layers on Ru(0001) [7], or contains other influences (see also below) as well is not clear without theoretical analysis.

So in view of the success of surface band structure considerations for the corresponding processes on metal surfaces [14, 16, 18], a comparison to the surface band structures of Si(100) and H–Si(100) suggests itself. Theoretical band structure calculations have been reported for both Si(100) [24] and H–Si(100) [25]. They indeed show that for both surfaces high densities of states (DOS) and a rather complicated situation of the empty bands exist in the energy range between 2.5 and 0.5 eV below the vacuum level, while at lower energies there are few states. Our structure in the CT times might then be related to the flat regions of the Δ_1 and Δ_5 bands [24, 25]. At lower energies the DOS is much lower, which can explain the longer CT times there (which we see clearly only for Si–H). While the possible uncertainty of up to ± 0.3 eV in the energy line-up weakens this conjecture somewhat, and the symmetry and surface projection of the band states and their overlap with the Ar^{-1} 4s have to be considered as well [14, 16, 18], a correlation with the band structure of the substrate is still the most likely explanation. An examination of this tentative conclusion and a detailed assignment needs theoretical work similar to these references, which would analyze the k-dependent transfer probabilities, to check this appealing interpretation. Such work would in reverse corroborate that direct CT from the ‘K’ 4s to the substrate governs the process seen.

On the other hand, the overall very short CT times are indeed unexpected and call for a discussion of possible other influences leading to sufficient overlap. Very fast CT from a larger molecule into a semiconductor has been seen before ([26] and references therein), but slower CT has also been reported [5]. The expectation of longer CT times on a semiconductor stems from the notions that bonding of Ar on a semiconductor is expected to be weaker than on a metal, and that there is a positive connection of bonding and coupling. It is interesting that the latter connection is not necessarily correct. In a theoretical paper Gauyacq and Borisov [27] have shown that for core-excited Ar on Cu(111) the CT time of the excited 4s electron does not continuously decrease with decreasing distance from the surface (which can be connected to the surface distance of the ground state atom and thus to its bond strength) but can have a maximum at a certain distance and decrease for further approach. This is due to their finding that the ‘4s’ orbital is not a pure s orbital but contains $4p_z$ admixture, and that the latter is increasingly polarized away from the surface upon decreasing the distance. This leads to smaller overlap and higher CT times. In our context, it means that the fastest CT need not be connected to the closest approach, i.e. strongest adsorption bond. We surely cannot claim that this effect does contribute here, and we emphasize that in the mentioned calculation [27] the absolute CT times come out considerably larger than measured here. Nevertheless, this stresses that simple arguments are not necessarily correct. A careful theoretical analysis would be very valuable.

We further note that the fact that screening times [28] in semiconductors are longer than the CT times seen here are no argument against short transfer times, as a transferred hot electron could well start out ballistically. This might weaken the connection to stationary band structure, but the importance of overlap of the Ar c^{-1}4s orbital with substrate surface orbitals would prevail. On the other hand, the complications introduced for the evolution of the excited electron delocalized from the Ar c^* atom may contain very interesting physics and would therefore again call for detailed theoretical scrutiny. Theoretical analysis of the initial stages of screening in

metals has shown very interesting effects *en route* to the development of a coupled response [29] which depend strongly on electron density. An experimental investigation of this evolution in the attosecond range by half-cycle radiation [6] would be extremely interesting. In this connection, we want to emphasize that the use of the term 'CT time' for the general process of the evolution of the initially localized excited electron should not be taken as containing any preoccupation with a particular mechanism.

Another feature of the data deserves a brief discussion. As obvious from figure 5 and by comparison with the inset of figure 1, the local structure of the CT results in the area of high quality data (from about 0.4 eV below to the same value above the resonance for Si–H) looks quite similar to the XAS curve (which is tracked by both the Auger and the Raman intensities; see top of figure 5). This has been seen in some cases before, e.g. for Ar on Pt(111) [12], while in many others [7, 14] the behavior is quite different. It might be connected to the band structure as well, even though this would require an accidental alignment of bands. We want to stress that this cannot be caused by the detuning influences, known from the ARR effect [30], being operative after all. While a symmetric variation of CT times around the resonance would then indeed be expected, the influence would be *opposite* to the one observed [30, 31]. If the decay *after* CT were—contrary to theory [15]—also a coherent process, then detuning from resonance (effectively decreasing the spectrum formation time for the one-step process) would decrease the chance for CT, as time shortening by detuning would *disfavor* CT. So the Raman fraction should be *lowest* on resonance [13], not have a (local) *maximum* as seen here. We want to stress that there is definitely no influence of the data analysis which could lead to the observed result—all spectra were analyzed independently, and as the signal strength goes down off-resonance, both contributions go down. So, while the signal-to-noise level gets worse, no systematic weighting of either component can occur. This aspect of the data is thus robust, and its reason worth theoretical scrutiny.

5. Summary and conclusions

Summarizing the results, we have obtained delocalization times of the Ar 4s excited electron of the Ar $2p_{3/2} \rightarrow 4s$ resonance of adsorbed Ar monolayers on n- and p-type Si(100), for the monohydride-covered surface and (to a lesser extent) the clean surface. The type of doping has no influence on the spectra, apart from a shift of the Fermi level. The localized 4s resonance of the quasipotassium Ar c^* atom is tied to the vacuum level and therefore independent of the doping. Peak shifts between the two surfaces, Si–H and Si–cl, for the photoelectron and decay spectra can be explained by different polarization screening of the excitations. Decomposing and analyzing the sets of decay spectra, we find CT times in the range 1.2–2.5 fs for Si–H, i.e. in the same range as for metal surfaces investigated previously, which is surprisingly short. There is a general decrease of about a factor of 2 for CT times on Si–cl versus Si–H. The Si–H data are very clean and sit on a very low background; their analysis is undebatable showing that the generally small CT times must be correct. They yield distinct structure in a certain energy range which is identical for n- and p-type surfaces. On the clean Si surfaces, the data are less extensive and less distinct, but may contain similar structure in the overlapping energy range. In line with all Ar/metal data analyzed theoretically before, a correlation to the empty band structure of Si(100) and H–Si(100) appears suggestive, with CT being fast for energies corresponding to high effective surface density of states of favorable symmetry and extension, as expected from a general overlap argument. The observed delocalization processes of the

locally excited electron are then due to CT into the substrate, in agreement with the impossibility of lateral CT because of the negative electron affinity of Ar. However, the unexpectedly short delocalization times do call for a more general examination of the processes connected with CT at semiconductor surfaces. Theoretical treatment would therefore be highly desirable. Also, experimental investigations of the detailed time evolution of the excited electron with attosecond time resolution would appear extremely interesting.

Acknowledgments

We thank Professors Th Fauster, J Pollmann and M Weinelt for informative discussions about the band structures of Si(100) and Si–H(100), P Feulner and M Weinelt about the problems of absolute energy calibrations at Si samples and J P Gauyacq for calling attention to possible polarization effects.

This work, which has been carried out in an international collaboration, has been supported by an EC general grant to Elettra and EC travel grants to DM, KK and GT. DM is grateful to the German Fonds der Chemischen Industrie for general support and GZ thanks the ICTP Trieste for financial support under the TRIL Programme.

References

[1] Dai H-L and Ho W 1995 *Laser Spectroscopy and Photochemistry on Metal Surfaces* vol 1 and 2 (Singapore: World Scientific)
[2] Menzel D 2006 *Surf. Interface Anal.* **38** 1702
[3] Petek H and Ogawara S 2002 *Annu. Rev. Phys. Chem.* **53** 507
[4] Frischkorn C and Wolf M 2006 *Chem. Rev.* **106** 4207
[5] Gundlach L, Ernstorfer R and Willig F 2007 *Appl. Phys.* A **88** 481
[6] Goulielmakis E, Yakovlev V S, Cavalieri A L, Uiberacker M, Pervak V, Apolonski A, Kienberger R, Kleineberg U and Krausz F 2007 *Science* **317** 769
[7] Wurth W and Menzel D 2000 *Chem. Phys.* **251** 141
[8] Brühwiler P A, Karis O and Martensson N 2002 *Rev. Mod. Phys.* **74** 703
[9] Menzel D 2008 *Chem. Soc. Rev.* **37** 2212
[10] Wurth W, Schneider C, Treichler R, Umbach E and Menzel D 1987 *Phys. Rev.* **35** 7741
[11] Karis O, Nilsson A, Weinelt M, Wiell T, Puglia C, Wassdahl N, Martensson N, Samant M and Stöhr J 1996 *Phys. Rev. Lett.* **76** 1380
[12] Keller C, Stichler M, Comelli G, Esch F, Lizzit S, Menzel D and Wurth W 1998 *Phys. Rev.* B **57** 11951
[13] Föhlisch A *et al* 2003 *Chem. Phys.* **289** 107
[14] Vijayalakshmi S, Föhlisch A, Hennies F, Pietzsch A, Nagasono M, Wurth W, Borisov A G and Gauyacq J P 2006 *Chem. Phys. Lett.* **427** 91
[15] Gortel Z W and Menzel D 2001 *Phys. Rev.* B **64** 115416
[16] Sanchez-Portal D, Menzel D and Echenique P 2007 *Phys. Rev.* B **76** 235406
[17] Keller C, Stichler M, Comelli G, Esch F, Lizzit S, Wurth W and Menzel D 1998 *Phys. Rev. Lett.* **80** 1774
[18] Föhlisch A, Feulner P, Hennies F, Fink A, Menzel D, Sanchez-Portal D, Echenique P M and Wurth W 2005 *Nature* **436** 373
[19] Gokhale S, Fink A, Trischberger P, Eberle K and Widdra W 2001 *J. Vac. Sci. Technol.* A **19** 706
[20] Higashi G S, Chabal Y J, Trucks G W and Raghavachari K 1991 *Appl. Phys. Lett.* **58** 1656
[21] Gadzuk J W 1975 *J. Vac. Sci. Technol.* **12** 289

[22] Camilloni R, Zitnik M, Comicioli C, Prince K C, Zacchigna M, Crotti C, Ottaviani C, Quaresima C, Perfetti P and Stefani G 1996 *Phys. Rev. Lett.* **77** 2646
[23] Weinelt M, Kutschera M, Schmidt R, Orth Ch, Fauster Th and Rohlfing M 2005 *Appl. Phys.* A **80** 991
[24] Kentsch C, Kutschera M, Weinelt M, Fauster Th and Rohlfing M 2001 *Phys. Rev.* B **65** 035323
[25] Wang M-P, Rohlfing M, Krueger P and Pollmann J 2006 *Phys. Rev.* B **74** 155405
[26] Duncan W R, Stier W M and Prezhdo O V 2005 *J. Am. Chem. Soc.* **127** 7941
[27] Gauyacq J P and Borisov A G 2004 *Phys. Rev.* B **69** 235408
[28] Leitenstorfer A, Huber R, Tauser F and Brodschelm A 2003 *Phys. Status Solidi* b **238** 455
[29] Borisov A, Sanchez-Portal D, Diez Muino R and Echenique P M 2004 *Chem. Phys. Lett.* **387** 95
[30] Gel'mukhanov F and Agren H 1999 *Phys. Rep.* **312** 87
[31] Gortel Z W, Teshima R and Menzel D 1998 *Phys. Rev.* A **58** 1225